Coherent structures in plumes with and without off-source heating using wavelet analysis of flow imagery

R. Narasimha, V. Saxena, S.V. Kailas

Abstract Laser flow visualization using fluorescent dye provides instantaneous snapshots of dye concentration across selected sections of the flow. We demonstrate the potential power of wavelet analysis in revealing the nature of organization present in such pictures of turbulent shear flows, in a case where it is difficult to discern any such organization in the raw image. The technique consists of examining the contours of the transform coefficients using two-dimensional wavelets on the raw image. It is applied here to diametral cross sections of a plume with and without off-source heating. It is found that in the unheated plume there is definite evidence for a sinuous large-scale ring-like organization, which, however, is absent when the off-source heating is switched on. The proposed technique not only enables eduction of coherent structures in flow-visualization pictures, but can also provide a wealth of scale-specific information on flow structure.

1
Introduction

Over the last decade, a series of experimental and numerical studies have been reported on the effect of appreciable quantities of volumetric heating on the development of turbulent jets and plumes (e.g. Bhat and Narasimha 1996; Basu and Narasimha 1999; Venkatakrishnan et al. 1998, 1999). The heat is injected between specific stations in the flow. The motivation for the studies

R. Narasimha (✉)
Fluid Dynamics Unit,
Jawaharlal Nehru Centre for Advanced Scientific Research,
Jakkur Campus, Bangalore 560 064
E-mail: roddam@caos.iisc.ernet.in

R. Narasimha
National Institute of Advanced Studies, Bangalore 560 012

V. Saxena
Indian Institute of Technology, Kharagpur 721 302

S.V. Kailas
Siemens Information Systems Ltd,
84 Keonics Electronics City, Hosur Road, Bangalore 561 229

has been both technological (e.g. combustion) and meteorological. In particular, attempts have been made to understand the fluid dynamics of clouds, where condensation of water vapour releases enough latent heat into the flow that it may be expected to significantly influence flow development. This expectation is borne out by the studies cited above.

In such flows, the entrainment of ambient fluid by the flows is of great interest. This is particularly true in the case of geophysical flows; for example, there is a long history behind the problem of entrainment in cumulus clouds (see Bhat and Narasimha 1996 for a discussion). A variety of earlier studies explored the issue of entrainment (for example, Morton et al. 1956; Turner 1973, 1986; Townsend 1976; Hunt 1993). Much of this work was inspired by a hypothesis first proposed by GI Taylor. According to this hypothesis the radial in-flow velocity into a free turbulent shear flow at any station is proportional to a characteristic velocity within the flow at that station. This characteristic velocity is usually taken as the local time-averaged maximum mean velocity at the level of the inflow. However, if the flow is self-preserving, different velocity scales are proportional to each other so that the precise choice made is not important. In general, these models predict that when buoyancy is enhanced at and beyond a certain station in the flow, as happens, for example, in the case of clouds consequent to the release of latent heat of condensation, the entrainment increases. However, all the evidence of cumulus clouds suggests that there is little or no lateral entrainment. In fact, the so-called tall cumulus tower (see e.g. Riehl 1979) looks conspicuously different from the usual turbulent jet or plume because the cloud does not spread laterally in the way that turbulent shear flows normally do.

The motivation for studying flows with off-source heating is to attempt to shed light on these strange entrainment characteristics of cloud-like flows. Experiments conducted by Bhat and Narasimha (1996) showed that heat addition does actually reduce entrainment and may even arrest it. On the basis of the laser flow visualization pictures that they took in this flow, they concluded that the dramatic effect on entrainment in flows with heat addition occurs because coherent structures present in the unheated flow are disrupted, or even destroyed, by the heat addition. It is useful to think of the entrainment process into the shear flow as consisting of three stages: (i) the initial stage of engulfment, during which ambient fluid is drawn into the core flow; (ii) the second stage, often called stirring but perhaps better termed 'mingling' (following

Narasimha and Venkatakrishnan 1999); and (iii) mixing, which is a diffusive molecule-to-molecule interaction. In this use of the terms we make a distinction between mingling, which could be a result of advective chaos and is not a space-filling process, and mixing, which is irreversible and space-filling. The suggestion of Bhat and Narasimha (1996) was therefore that the entrainment was arrested at the very first stage of engulfment itself. The consequent differences in mingling were addressed in Narasimha and Venkatakrishnan (1999).

All of this work confirms that coherent structures play a crucial role in determining the character of the entrainment into the flow. Extensive studies have been made of coherent structures in the last 30 years and have been reviewed by Hussain (1986) and Fiedler (1988). Problems, however, still remain in educing the coherent structures in the flow; a variety of techniques have been described in the literature. Earlier work (for example, Roshko 1976) depended on very clear visual evidence in pictures taken of the flow. In flows where the organization is strong this technique works very well. However, it is well known that in jets and plumes the coherent structure cannot be so easily discerned in straightforward flow visualizations. Measurements of the two-point space–time correlation of longitudinal velocity fluctuations (Tso and Hussain 1989) provide very useful quantitative information. It is possible that such methods underestimate the degree of order present because of the problems associated with averaging over an ensemble of rather jittery structures, especially as it is well known that both spatial and temporal scales of such structures can be highly variable. This is clear, for example, from the data provided by Bernal (1988) on mixing layers. Furthermore, if there is more than one type of structure in the flow, such techniques can become quite complicated and will demand some knowledge of the types of structures that occur before suitable correlation configurations can be designed.

With the availability of high-quality flow imagery from laser-based techniques (e.g. Dahm and Dimotakis 1990) or from direct numerical simulations, various signal-processing techniques may be used to help reveal the structure in the flow. A wavelet analysis of axial sections of a turbulent jet was presented by Everson et al. (1990). In our laboratory, we have for some years been exploring the use of wavelets as signal-processing techniques in many applications. A preliminary application to diametral sections of a jet flow was made by Kailas et al. (1995) using a thresholding technique on the wavelet transform coefficient. Cutler and Johnson (1997) also used a thresholding technique for analysing images of a plume to study the nature of intermittency in a supersonic flow with injection. Kailas and Narasimha (1999) used wavelets to study mixing layers, with a view to calibrate the technique in a flow in which the nature of the coherent structure is already well known. Their study shows that with a careful use of wavelet techniques, very useful information can be obtained on the structure of the flow over a wide range of spatial scales.

In order to make this paper comprehensible, we briefly recapitulate the main features of the experimental set-up used in our studies and the wavelet technique adopted by Kailas and Narasimha (1999). We then illustrate the kind of conclusions on coherent structures that can be obtained by this technique through an analysis of two images acquired experimentally.

2
Experiments

We shall here examine chiefly the imagery acquired in a plume subjected to off-source heating (Venkatakrishnan et al. 1998, 1999). A schematic of the flow configuration and the experimental arrangement is shown in Fig. 1; more details can be found in the references cited, and in Bhat and Narasimha (1996). The plume is generated at the bottom of a water tank of dimensions $600 \times 600 \times 1200$ mm^3, by means of an electric heater enclosed inside an acrylic box. The tank is filled with filtered and deionized water to ensure a nonconducting ambient fluid. The active fluid (deionized water rendered electrically conducting by the addition of hydrochloric acid) is supplied to the plume-heating chamber by means of a variable-height constant-level tank. The temperature difference between plume and ambient at nozzle exit is maintained at 55°C by appropriate variation of the voltage supplied to the heater and of the height of the constant-level supply tank. The exit buoyancy flux is constant to within ±2% over the duration of the experiment (typically 15–20 min), as inferred from measurements of the velocity and temperature at the nozzle exit. The diameter d of the nozzle from which the plume issues is 4 mm, and the exit velocity U_0 is 0.16 m s^{-1}. This gives a Reynolds number Re of 670 based on exit velocity and diameter. Since the buoyant fluid has some initial momentum (it is a so-called forced plume), the flow behaves like a jet near the nozzle exit and a plume farther downstream (Fisher et al. 1979). It is known from the work of Papanicolaou and List (1988) that the plume regime
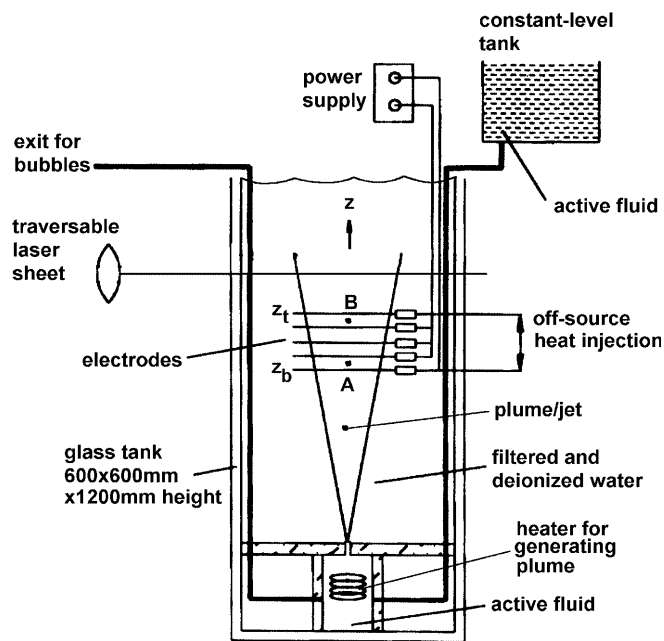
Fig. 1. Experimental set-up. The plume is generated by the heater at the bottom of the tank, off-source heating is injected through five electrodes. Analysed flow sections were taken at station B

prevails at an axial distance beyond $z=5\ell_M$, where ℓ_M, the Morton length scale, is ~16 mm or $4d$ in the present experiments. The flow is therefore expected to behave like a plume beyond $20d$.

The enhancement of buoyancy is achieved by the volumetric heat-injection method developed by Bhat et al. (1989). Electrodes made of fine platinum wire, netted on a thin rectangular supporting frame, are placed horizontally across the flow at desired heights. Wire Reynolds numbers are below 10, so the mechanical disturbance to the flow caused by the wires is negligible. A high-frequency (20 kHz) alternating voltage is applied between the electrodes. The acid concentration in the plume is a proxy for the water vapour in the clouds, making the present technique more relevant to clouds than earlier experiments, which depended on chemical reactions (and hence on the very mixing that is the object of study) for heat generation.

The amount of heating Q, which can go up to 1000 W, is easily controlled by varying the voltage (over the range 0 to 250 V) across the electrodes. Heat is added over the region from $z=50d$ to $z=80d$ in the present experiments. Since we expect the flow to behave like a self-similar plume beyond $20d$, this choice of the location of the heat-injection zone ensures that the flow has the properties of a fully developed plume before being subjected to the volumetric heating.

The structural differences in the flow are examined by visualizing the flow using the laser-induced fluorescence technique, with rhodamine 6G dye and a 300-μm thick laser sheet from a 4-W argon ion laser as the light source. Still photographs were taken with a Canon EOS 1000 still camera, and video recordings were taken with a National (model NV-M5EN) VHS video camera. The laser is actually a part of an LDV system, but no velocity data are directly utilized in this study.

For the sake of simplicity the plume with and without off-source heat injection will be referred to as the 'heated plume' and 'unheated plume', respectively.

3
Methodology

The basic methodology used here, following Kailas and Narasimha (1999), is to examine the two-dimensional (2D) wavelet transform of a flow image at various scales. The basic variable is the gray-scale intensity of the image $f(\boldsymbol{x})$, where $\boldsymbol{x}$ is the two-dimensional vector locating position in the image.

The wavelet transform $\hat{f}(\mathbf{x}, a)$ of this function $f(\boldsymbol{x})$ is defined as the convolution product of a scaled and shifted mother wavelet $\psi(\boldsymbol{x})$ with $f(\boldsymbol{x})$:

$$\hat{f}(\mathbf{x}, a) = \frac{1}{a} \int f(\mathbf{x}\prime)\psi\left(\frac{\mathbf{x} - \mathbf{x}\prime}{a}\right) \mathrm{d}\mathbf{x}\prime \; , \qquad (1)$$

where a is the scale parameter and $\boldsymbol{x}'$ the shift parameter; $\mathrm{d}\boldsymbol{x}'$ is an element of image area. Extensive treatment of wavelet transform principles and techniques are now available in various books (e.g. Strang 1989; Meyer 1993). We need to note here that to be 'admissible' the mother wavelet $\psi(\boldsymbol{x})$ must be a rapidly decaying function of its argument (i.e. must have compact support), have a zero mean, and be normalized suitably, usually to ensure

invertibility and preservation of the L^2 norm. Several functions meeting these criteria are available in the wavelet literature. Both discrete and continuous versions of the wavelet transform are possible. For the present work, we follow Kailas and Narasimha (1999) and prefer the continuous version, which, although richly redundant, facilitates analysis. This is because of the freedom it provides on the choice of wavelet scale. Basically, as one can see from Eq. (1), the continuous wavelet technique maps the original field into a single-parameter family of transform fields. In addition, it can identify *localized* regions of 'energy' concentration, which is its major advantage over conventional Fourier-type analysis. The word 'energy' here does not necessarily denote a mechanical quantity, but rather a measure of the activity of the variable under consideration. Thus, in the case of the images analysed here, this implies the possibility of detecting regions of high activity in dye concentration at different physical scales.

The transform was previously used to study coherent structures in turbulence. Thus Farge (1992) reconstructed scale-specific regions of high vorticity concentration in direct numerical simulations by inverting the transform and used it to study the dynamics of these structures. We use the transform solely as a powerful filter and hence detector of structures at various spatial scales.

The mother wavelet we adopt is the 2D Mexican hat,

$$\psi(\mathbf{x}) = \left(2 - x^2 + y^2\right) \exp\left[-\left(x^2 + y^2\right)/2\right] \; , \qquad (2)$$

where $\boldsymbol{x} \equiv (x,y)$. The zero-crossings of this transform have been shown to be particularly useful in detecting regions of sharp gradients in an image (Marr 1982). Such gradients may assist in identifying the interfaces between coherent and noncoherent motion. A threshold of 30 (on a gray-level scale of 256) has been applied to eliminate noise in the original photographic images. Other processing details are as in Kailas and Narasimha (1999).

For better appreciation of the physical scales of the structures detected, in the present study we replace the scale a of the wavelet transform by a', the ratio of the wavelet scale to the length L, along either axis, of the images described in Sect. 4.

4
Results

Using the set-up described in Sect. 2, a variety of flow visualizations as well as velocity measurements have been made and reported elsewhere (Venkatakrishnan et al. 1998, 1999). The visualizations covered both axial and diametral sections.

For the demonstration of the power of the wavelet technique described in Sect. 3, we concentrate here on diametral images. In particular, we analyse cross sections of the plume located towards the top of the heat-injection zone, shown as station B (z/d=79.4) in Fig. 1. The raw data for the present analysis are contained in the two flow visualization images, without and with heating, respectively, acquired by Venkatakrishnan et al. (1998) and reproduced in Fig. 2. The flow conditions correspond to a plume Reynolds number of 670 and an off-source heat input of 555 W. It will be agreed, we believe, that unlike in the well-known pictures of the mixing layer (e.g. Roshko 1976),
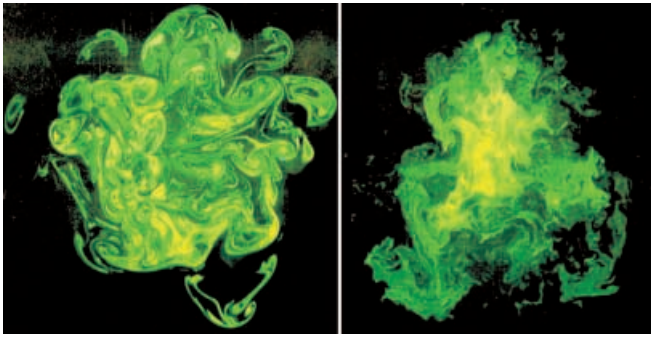
Fig. 2. Laser-induced fluorescence images of sections of plume at z/d=79.4: (*left*) unheated, (*right*) heated, heat input=555 W (from Venkatakrishnan et al. 1998)

there is no discernible order in either of the images of Fig. 2. However, a qualitative difference between them is evident, as we shall more explicitly describe below.

Before presenting the results of the wavelet analysis, we briefly describe how the original photographs of laser fluorescence in the flow were processed. First the photographs were scanned using a digital scanner (UMAX Powerlook 2000) and saved as 256-colour bitmap images. These images were then converted into 256 gray-scale images using Adobe Photoshop 5. The images were then digitized and saved as data files (368×392 pixels and 280×300 pixels for unheated and heated plumes, respectively) by storing the palette number of each point in the gray scale. The images obtained in this manner contain some noise. Since transformed images at small scale are particularly sensitive to such noise, various methods such as thresholding were tried to eliminate it. This was particularly necessary in the case of the heated plume, where the edges were not so clear.

Wavelet transformation was applied to the raw images at different values of a'. Results are presented at six wavelet scales, which cover small, intermediate, and large flow scales. Wavelet images at all scales are available at the web page of R.N. at http://www.jncasr.ac.in/fdu/rnsimha/plume.mpg, where an animation of the images is available with time representing the wavelet scale a'.

In the unheated plume (Fig. 2) some ambient fluid is clearly visible in the core of the plume: there are regions near the axis with low dye concentration. Eddies extend into and engulf the ambient fluid in the active region. In the heated plume, on the other hand, the dye is more homogeneously mixed in what we shall call the 'core' region, where little ambient fluid is visible. Furthermore, the eddies do not extend into the ambient fluid. While the boundaries are relatively sharp and highly convoluted and fractal in the unheated plume, the edges are not so sharply defined or convoluted in the heated plume. It will be noted that while the unheated plume displays more 'structure' in some sense, neither of the two images reveals any easily discernible degree of coherence or organization.

We now discuss the wavelet transform maps at different scales, shown in Fig. 3. Figure 3a is the raw image of Fig. 2, but is colour-coded for ease in comparison with the wavelet transforms. Figure 3b–f shows basically colour-coded contour intervals of wavelet transform coefficients

at selected scales. Figure 3b shows the wavelet transform at scale a'=0.02. In the unheated plume positive and negative values (red and green) are distributed across the image. In the heated plume one can recognize a sparse area of near-neutral coefficients, indicating low mingling activity and corresponding to the nearly homogeneous core of Fig. 3a. This core is surrounded by a denser region of both red and green where the activity is greater. On the whole, the broad conclusions from Fig. 3b are consistent with what one may infer from Fig. 3a.

At scale a'=0.14 (Fig. 3c), the filamentary shape of the areas of activity is clearly seen; it must, of course, be remembered that we are looking only at a diametral section, so nothing can be said about the third dimension of the structures, which can therefore be (in principle) sheet-like perpendicular to the plane of the image. In the unheated plume activity seems to be moving away from the centre. In the heated plume the signature of the core can now be barely discerned, and, in fact, red and green are more homogeneously distributed across the image. Furthermore, the structures show greater connectivity or less fragmentation (i.e. fewer isolated 'spots' of red or green) than in the unheated case. The two flows are clearly stirred differently.

Figure 3d shows the transforms at the scale a'=0.28. In the unheated plume a void is developing in the central region, and the outward movement of the active region, seen already in Fig. 3c, is confirmed. In the heated plume, on the other hand, the core is becoming predominantly red. The obvious interpretation is that, at this scale, the flow is best seen as separating into a (nearly homogeneous) core and a more active periphery. We can say that there appears to be more mingling and mixing outside the core in the heated plume.

Figure 3e (scale a'=0.51) begins to reveal a ring-like organization in the unheated plume: the central region is again a void, and outside the red ring is a green periphery. Thus a three-region separation is beginning to emerge. In the heated plume there is again the red core – now rather elongated – and a green periphery, with some spotty regions in the neighbourhood of the core.

Finally, in Fig. 3f (scale a'=0.80), a sinuous or fluted ring-like structure of the unheated plume is clearly seen, with the void inside and a green outer band. Note, however, the high spots within each of the outer regions: the ring is not completely axisymmetric, but has five (or possibly six) lobes. These lobes are reminiscent of the 'cells' that Basu and Narasimha (1999) reported in the vorticity field in a cross section of the jet, for which they provided direct numerical simulation results. This suggests that the spots on the outer edge may be signatures of large-scale engulfment and/or or mingling. The heated plume has clearly no ring-like structure at all.

5
Discussion
The main purpose of this paper is to demonstrate the potential power of wavelet transforms in analysing flow imagery for the purpose of inferring the nature of any organization or coherent structure present in the flow, especially in cases where no such organization is apparent
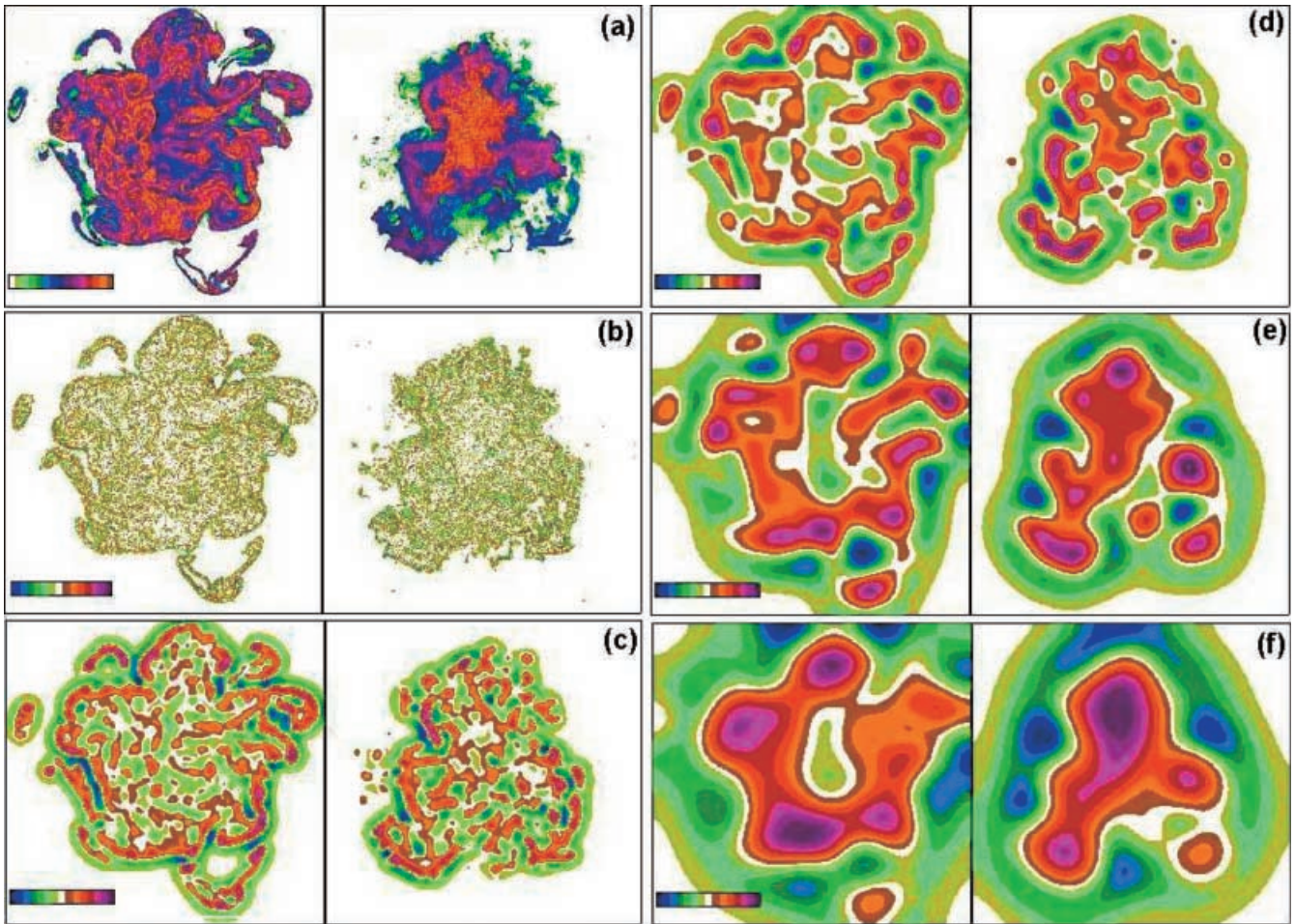
Fig. 3. Colour-coded contour intervals of wavelet transform coefficients of images in Fig. 2, (*left*) unheated, (*right*) heated: **a** colour-coded raw image; **b** a'=0.02; **c** a'=0.14; **d** a'=0.28; **e** a'=0.51; **f** a'=0.80

in the raw data or image. However, we must note that the strong presence of large-scale ring-like organization in the unheated plume, and its absence when heat is switched on, lends further support to the conclusion of Bhat and Narasimha (1996) that one of the major effects of volumetric heat injection in such a flow is the disruption, or even destruction, of the coherent structure present in the flow. The consequence of this effect is seen in the dramatic reduction (or even cessation) of entrainment from the ambient on the injection of heating.

We must also point out that a ring-like structure in a diametral section of a round (unheated) jet was also observed in the preliminary wavelet analysis of laser visualizations by Kailas et al. (1995). We show part of the evidence in Fig. 4, which displays a thresholded wavelet transform of a cross section of the jet. (The image analysed was again a laser-induced fluorescence, taken in the same apparatus as described in Sect. 2: z/d=30, jet nozzle diameter d=8 mm, Reynolds number at the nozzle exit Re=1500.) The organization into a five- or six-lobed ring is once again clear. However, the present technique of examining contour plots after an initial application of a low threshold to remove noise is much more revealing and effective.

In both plume and jet we have only analysed diametral sections, so the character of the structure in the axial

dimension needs yet to be determined. However, the present findings are consistent with the conclusions of Siddhartha et al. (2000), based on a similar wavelet analysis of direct numerical simulations of unheated and heated jets carried out by Basu and Narasimha (1999). The proposal of Siddhartha et al. is that the coherent structure consists of a toroidal base with a sheet of vorticity wrapping above it, rather like a cone. A section of this
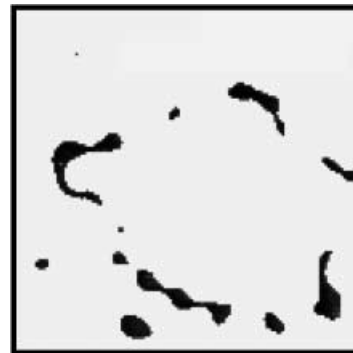
Fig. 4. High-threshold (level 600) wavelet transform of unheated round jet at wavelet scale a'=0.32, cross section at z/d=30, d=8 mm, Re=1500 (from Kailas et al. 1995

turban-like structure, hollow inside because there is little vorticity in the middle, would be expected to reveal a ring of the kind found in the present study.

6
Conclusions

The power of wavelet analysis is seen in the way that the ring-like structure hidden in the raw data of Fig. 2 is revealed in Fig. 3f. It must be emphasized that this ordered structure is derived from an instantaneous snapshot, and not by any kind of averaging technique. For a complete understanding of the nature and history of the coherent structures in a flow, it is necessary to examine movies of wavelet transforms (at each wavelet scale) of imagery in different sections of the flow. This is a project on which the authors are currently working; results will be reported in the near future.

References

Basu AJ, Narasimha R (1999) Direct numerical simulation of turbulent flows with cloud-like off-source heating. J Fluid Mech 385:199–228

Bernal LP (1988) The statistics of the organised vortical structure in turbulent mixing layers. Phys Fluids 31:2533–2543

Bhat GS, Narasimha R (1996) A volumetrically heated jet: large-eddy structure and entrainment characteristics. J Fluid Mech 325:303–330

Bhat GS, Narasimha R, Arakeri VH (1989) A new method of producing local enhancement of buoyancy in liquid flows. Exp Fluids 7:99–102

Cutler AD, Johnson CH (1997) Analysis of intermittency and probe data in supersonic flow with injection. Exp Fluids 23:38–47

Dahm WJA, Dimotakis PE (1990) Mixing at large Schmidt number in the self-similar far field of turbulent jets. J Fluid Mech 217:299–330

Everson R, Sirovich L, Sreenivasan KR (1990) Wavelet analysis of the turbulent jet. Phys Lett A 145:314–322

Farge M (1992) Wavelet transforms and their applications to turbulence. Ann Rev Fluid Mech 24:395–457

Fiedler HE (1988) Coherent structures in turbulent flows. Prog Aero Sci 25:231–270

Fisher HB, EJ List, RCY Koh, J Imberger, NH Brooks (1979) Mixing in Inland and Coastal Waters. Academic, San Diego, Calif

Hunt JCR (1993) Atmospheric jets and plumes. In: Davies PA, Valente MJ (eds) Recent Research Advances in the Fluid Mechanics of Turbulent Jets and Plumes, Proc. NATO Advanced Study Institute, Viano di Castello, Portugal. Kluwer, Dordrecht, pp 309–334

Hussain AKMF (1986) Coherent structures and turbulence. J Fluid Mech 173:303–356

Kailas SV, Narasimha R (1999) The eduction of structures from flow imagery using wavelets. I. The mixing layer. Exp Fluids 27:167–174

Kailas SV, Bhat GS, Kalavathi K (1995) On coherent structures in a round turbulent jet educed by wavelet transforms. In: Chew YT, Tso CP (eds) Proc 6th Asian Cong Fluid Mech, Singapore, pp 993–997

Marr D (1982) Vision. Freeman, New York

Meyer Y (1993) Wavelets: Algorithms and Applications. SIAM, Philadelphia

Morton BR, Taylor GI, Turner JS (1956) Turbulent gravitational convection from maintained and gravitational sources. Proc Roy Soc A 234:1–23

Narasimha R, Venkatakrishnan L (1999) The reduction in 'mingling' with ambient fluid in a jet with off-source heating. In: Proc Eighth Asian Congress of Fluid Mechanics, Shenzhen, China, 6–10 December, pp 275–278

Papanicolaou PN, List EJ (1988) Investigation of round vertical buoyant jets. J Fluid Mech 195:341–391

Riehl, H (1979) Climate and Weather in the Tropics. Academic, New York

Roshko A (1976) Structure of turbulent shear flows: a new look. AIAA J 44:1349–1357

Siddhartha SS, Narasimha R, Basu AJ, Kailas SV (2000) Coherent structures in numerically simulated jets with and without off-source heating. Fluid Dyn Res 26:105–117

Strang G (1989) Wavelets and dilation equations: a brief introduction. SIAM Rev 31:614–627

Tso J, Hussain F (1989) Organised motions in a fully developed turbulent axisymmetric jet. J Fluid Mech 203:425–448

Turner JS (1973) Buoyancy Effects in Fluids. Cambridge University Press, Cambridge

Turner JS (1986) Turbulent entrainment: the development of entrainment assumption and its application to geophysical flows. J Fluid Mech 173:431–471

Townsend AA (1976) The Structure of Turbulent Shear Flow, 2nd edn. Cambridge University Press, Cambridge

Venkatakrishnan L, Bhat GS, Prabhu A, Narasimha R (1998) Visualization studies of cloud-like flows. Curr Sci 74:597–606

Venkatakrishnan L, Bhat GS, Prabhu A, Narasimha R (1999) Experiments on a plume with off-source heating: implications for cloud fluid dynamics. J Geophys Res 104:14,271–14,281